

Environmental assessment of biofuel pathways in Ile de France based on ecosystem modelling, including land-use change effects

Benoît Gabrielle, Nathalie Gagnaire, Rea Massad, Karine Dufossé, Cécile Bessou

► **To cite this version:**

Benoît Gabrielle, Nathalie Gagnaire, Rea Massad, Karine Dufossé, Cécile Bessou. Environmental assessment of biofuel pathways in Ile de France based on ecosystem modelling, including land-use change effects. *Bioresource Technology*, Elsevier, 2014, 152, pp.511-518. 10.1016/j.biortech.2013.10.104 . cirad-00938241

HAL Id: cirad-00938241

<http://hal.cirad.fr/cirad-00938241>

Submitted on 29 Jan 2014

HAL is a multi-disciplinary open access archive for the deposit and dissemination of scientific research documents, whether they are published or not. The documents may come from teaching and research institutions in France or abroad, or from public or private research centers.

L'archive ouverte pluridisciplinaire **HAL**, est destinée au dépôt et à la diffusion de documents scientifiques de niveau recherche, publiés ou non, émanant des établissements d'enseignement et de recherche français ou étrangers, des laboratoires publics ou privés.

1 Environmental assessment of biofuel pathways in Ile de France based on ecosystem

2 modelling, including land-use change effects

3

4 Benoît Gabrielle^{1,*}, Nathalie Gagnaire², Rea Massad², Karine Dufossé², C. Bessou³

5

6 1 :*AgroParisTech, INRA, UMR 1091 Environnement et Grandes Cultures, F-78850*

7 *Thiverval-Grignon, France.*

8 2 : *INRA, AgroParisTech, UMR 1091 Environnement et Grandes Cultures, Thiverval-*

9 *Grignon, France.*

10 3: *CIRAD, Performance of perennial cropping systems Research Unit, Av. Agropolis,*

11 *34398 Montpellier, France.*

12

13

14 * Corresponding author. Tel.: +33 1 30 81 55 51; Fax: +33 1 30 81 55 63

15 E-mail address: Benoit.Gabrielle@agroparistech.fr

16

17

18 **ABSTRACT**

19 The greenhouse gas (GHG) balance of biofuels largely hinges on the magnitude of nitrous
20 oxide (N₂O) emissions from arable soils during feedstock production, which are highly
21 variable. Here, used an agro-ecosystem model to generate these emissions at a high resolution
22 over the Ile-de-France region in Northern France, for a range of feedstocks. The emissions
23 were input to a life-cycle assessment of candidate biofuel pathways: bioethanol from wheat
24 and sugar-beet, biodiesel from oilseed rape, and ethanol from miscanthus.

25 Compared to the widely-used methodology based on fixed emission factors, ecosystem
26 modelling lead to 55% to 70% lower estimates for N₂O emissions, emphasizing the
27 importance of regional factors. The life-cycle GHG emissions of 1st generation biofuels were
28 50% to 70% lower than fossile-based equivalents, and 85% lower for cellulosic ethanol.
29 Indirect land-use change effects negated these savings for bio-diesel and wheat ethanol, but
30 were offset by direct effects for cellulosic ethanol.

31

32

33 **Keywords:** Biofuels, Energy crops, Greenhouse gas emissions, Land-use change,
34 Life-cycle assessment

35

36 **1. Introduction**

37 Controversy is still ongoing regarding the greenhouse gas (GHG) intensity of biofuels and
38 bioenergy chains in general (Kavanagh, 2006; Crutzen et al., 2008). While there appears a
39 consensus on the benefits of displacing fossil fuels with energy from biomass, at least when
40 excluding indirect land-use change (iLUC) effects (Farrell et al., 2006; Chum et al., 2011),
41 the GHG savings reported in the literature may differ widely for seemingly similar pathways
42 (Chum et al., 2011). These results are usually based on the life cycle assessment (LCA)
43 methodology, relying on the same international standards but different calculation hypotheses
44 and scope, in particular regarding co-product allocation methods, system boundaries,
45 functional unit, or impact characterization. However, correcting for these differences to make
46 these results commensurate only reduces part of their variability (Farrell et al., 2006). The
47 source of input data used in the inventory step of the LCA plays a major role in its final
48 outcome, in particular regarding crop management and biomass yields per unit area (Davis et
49 al., 2013). Also, the emissions occurring upon the cultivation of energy crops in the field have
50 a strong influence on the energy and GHG balances of the whole chain (Smeets et al., 2009).
51 For instance, the efflux of nitrous oxide (N₂O) resulting from fertilizer application accounted
52 for 20 to 40% of the GHG emissions of the 1st generation biofuels consumed in France
53 (ADEME, 2010), and depending on the methodology used this efflux could vary by a factor
54 of 2, according to the same study. Worldwide, Smeets et al. (2009) showed that this
55 uncertainty, when compounded with N₂O emissions related to land-use changes could alter
56 the life-cycle GHG emissions of biofuels by more than 50%, leading to higher emissions than
57 their fossil counterparts in some cases.

58 In most LCAs of bioenergy chains, N₂O emissions from soils are estimated with fixed
59 emission factors (EFs), expressing a proportionality between N₂O efflux and fertilizer N input

60 rates (Cherubini, 2010). However, these factors carry a large uncertainty. For instance on a
61 global scale, the EF for direct emissions of N₂O related to fertilizer N inputs to cropland
62 varies between 0.3% and 3%, with a median value of 1% (Eggleston et al., 2006). This
63 worldwide default value were recently questioned based on the gap between bottom-up
64 inventories of fertilizer-derived field emissions and the atmospheric build-up of N₂O (Crutzen
65 et al., 2008). The higher EFs proposed by the latter authors would negate the GHG benefits of
66 most bioenergy pathways, including 2nd generation biofuels from lignocellulose. It thus
67 appears crucial to obtain more reliable assessments of the level of N₂O emissions attributable
68 to bioenergy feedstock production (Cherubini, 2010).

69 Emissions of N₂O from soils are difficult to assess because they vary widely across time and
70 space, depending on environmental conditions (soil properties and climate) and agronomic
71 characteristics such as crop yields and management, and fertilizer use efficiency (Stehfest and
72 Bouwman, 2006). Improving their estimation implies taking these drivers explicitly into
73 account, and applying LCA at the supply area level rather than based on notional country- or
74 European-wide 'average' cultivation fields (Gabrielle and Gagnaire, 2008). This stresses the
75 need for developing generic methods with a capacity to address the variability within these
76 feedstock supply areas. Combining experimental monitoring of field-scale emissions with
77 biophysical models appears as a promising avenue to provide reliable estimates of N₂O
78 emissions at a scale relevant for bioenergy units (Dufossé et al., 2013). However, there has
79 been thus far very little work on the comparison of emission maps obtained with such bottom-
80 up estimates with top-down, integrative atmospheric measurements, such as tower fluxes.
81 Most top-down source inversion studies from atmospheric measurements have been carried
82 out at large scales, from continental to global, with a coarse resolution of terrestrial sources of
83 N₂O (Thompson et al., 2011).

84 The objectives of this paper were i/ to improve the estimations of field emissions of bioenergy
85 feedstocks, in particular nitrous oxide, by using ecosystem modelling at regional scale, and ii/
86 to examine the impact of using such estimates in lieu of fixed emission factors in the LCA of
87 current and prospective biofuel chains for the area. The modelling also made it possible to
88 take into accounts the effects of land-use-change scenarios on the outcome of the LCAs.
89 Here, we thus generated high-resolution maps of field emissions from in the Ile de France
90 region (Northern France), using an agro-ecosystem model, for use in the LCA of
91 representative biofuel chains for the area. The Ile de France region was selected because it
92 was within the catchment probed by the atmospheric measurements, and is also included a set
93 of field trials in Grignon (to the West of the domain) in which all the crops considered had
94 been tested (Gabrielle et al., 2012; Goglio et al., 2013). The maps of N₂O emissions of were
95 verified by using them as prior estimates in the inversion of the meso-scale atmospheric-
96 chemistry transport model CHIMERE, against concentrations recorded at various heights in
97 the planetary boundary layer at 2 sites to the South of Ile de France, for the year 2007
98 (Gabrielle et al., 2012). The maps were subsequently expanded to test various feedstocks
99 using a series of near-term future weather data to capture the effect of inter-annual variability
100 and the long-term effects of perennial crops over their growing cycle (typically 20 years). The
101 resulting fluxes were input into the life-cycle inventory of the following chains: biodiesel
102 production from oilseed rape; bioethanol production from winter wheat and sugar-beet (first-
103 generation biofuels); and bioethanol from *Miscanthus x giganteus* (a perennial C4 grass,
104 further referred to as miscanthus), representing a prospective second-generation pathway.
105 The effect of feedstock production on soil C balances and dynamics were included in the
106 LCA, relative to a reference land-use scenario in the absence of bioenergy production in Ile de
107 France, thus account for direct LUC effects. Indirect LUC was taken into account based on
108 the meta-analysis of De Cara et al. (2012).

109 **2. Materials and Methods**

110 *2.1 Biofuel feedstocks and pathways*

111 The biofuel value-chains considered included: bio-diesel from oilseed rape, ethanol from
112 sugar-beet and winter wheat, and cellulosic ethanol obtained by enzymatic hydrolysis from
113 miscanthus biomass. The baseline for the life-cycle inventory data was taken from a recent
114 study carried out by the French Environment Agency on biofuels and their fossile equivalents
115 in the context of France (ADEME, 2010). System boundaries included feedstock production
116 to a regional storage after conversion in a biorefinery, but included CO₂ emissions upon
117 combustion for fossile fuels.

118 The selected feedstock supply area was Ile de France, for which comparisons between
119 ecosystem modelling and top-down atmospheric measurements were available to infer N₂O
120 fluxes. Simple assumptions were made for direct land-use changes (LUC) related to feedstock
121 production. A recent study based on historical land-use data (In Numeri, 2012) concluded that
122 in France 1st generation biofuel crops mostly diverted existing crops from food to energy end-
123 uses, or displaced similar crops (eg, oilseed rape substituted pea crops). Only 13% of the
124 cropland area used for biofuel production was taken on set-aside land, and this occurred
125 mostly in regions outside of Ile de France. Therefore, direct LUC effects were neglected for
126 arable crops. For the perennial lignocellulosic crop (miscanthus), the assumption was that the
127 latter either displaced annual crops or was established on set-aside land. The associated direct
128 LUC effects were simulated by considering the differences between the emissions occurring
129 on the modelled miscanthus fields and those occurring in either the reference rotation of
130 arable crops or a continuous fallow. Compared to rotational fallow, the latter represented 40%
131 of the overall set-aside area in 2007, and were considered as a reference, conservative
132 scenario for conversion of set-aside cropland to miscanthus. For lack of an adequate

133 simulation model, continuous fallow was assumed to have the same C and N dynamics as the
134 miscanthus fields.

135 Indirect land-use changes at the global scale (ie the cascading effects related to the diversion
136 of food crops to fuel purposes) were accounted for in the GHG balance of biofuels based on
137 the median values reported by De Cara et al. (2012) in their meta-analysis of the literature on
138 this topic. The analysis accounts for biofuel type, feedstock type and production area, and we
139 used the set of values that were the most relevant to the biofuel chains evaluated here.

140 *2.2.2. Model simulations*

141 Crop yields, soil C dynamics and emissions of reactive N (Nr), including N₂O in particular
142 were simulated with the agro-ecosystem model CERES-EGC (Goglio et al., 2013) over the Ile
143 de France region. Briefly, CERES-EGC was adapted from the CERES family of soil-crop
144 models, with a focus on the simulation of environmental outputs such as nitrate leaching and
145 gaseous emissions of ammonia and nitrogen oxides. It contains submodels for the major
146 processes governing cycles of water, carbon and nitrogen in agro-ecosystem models. A
147 physical module simulates the transfer of heat, water and nitrates down the soil profile as well
148 as soil evaporation, plant water uptake, and transpiration in relation to climatic conditions. A
149 microbiological module simulates the turnover of organic matter in the plough layer,
150 involving both mineralization and immobilization of mineral N (denitrification and
151 nitrification). CERES-EGC includes a submodel that simulates the production of NO and N₂O
152 through the nitrification and denitrification pathways. The model was adapted to miscanthus
153 by explicitly introducing a rhizome pool and biomass translocation processes specific to
154 perennial crops from one growing season to the next (Picoche, 2012).

155 Ile de France may be approximated as a 150 km x 150 km square area surrounding Paris, with
156 55 % cropland. A GIS database was constructed with available geo-referenced data on this

157 region, including administrative borders, land-cover type, crop management practices, soil
158 properties and climate. The corresponding layers of spatial information were mostly in vector
159 format, and overlaid to delineate elementary spatial units representing unique combinations of
160 soil types, weather data, and agricultural management. These units were subsequently used in
161 the CERES-EGC simulations at the field-scale, in a bottom-up approach to map the
162 emissions, using the procedure detailed by Dufossé et al. (2013).

163 Since miscanthus is a perennial crop with a lifespan of up to 20 years, it was necessary to run
164 long-term simulations, and also to capture inter-annual variability effects and soil organic C
165 dynamics. We thus used weather data predicted for the 2010-2030 time slice by the DRIAS
166 project in France (Lémond et al., 2011), using the IPSL-CM4 model with the A1B GHG
167 emission scenario from IPCC, which appeared as an intermediate scenario for air temperature
168 and rainfall among the range of models and forcings tested by this project. Compared to the
169 1961-1990 period, air temperature would rise by 1.35 °C, with a average of 11.7 °C for the
170 2010-2031 time slice, and rainfall would remain level at an average of 641 mm yr⁻¹. CERES-
171 EGC was run for the current land-use (2010) and the various feedstocks and land-uses
172 hypothesized for biofuel production. For the verification year (2007), we used gridded
173 weather data from the MCRU data base (Chen et al., 2009), with a 0.25° x 0.25° resolution,
174 and cropland areas from the last available survey (pertaining to the year 2000).

175 An alternative, reference methodology for N₂O emissions was based on the 2006 IPCC
176 guidelines (Eggleston et al., 2006), as implemented in the baseline LCA (ADEME, 2010),
177 using the Tier 1 approach (ie default emission factors). Indirect emissions of N₂O due to
178 leaching were calculated as 0.75 % of the nitrate losses, simulated either with CERES-EGC or
179 expert knowledge (ADEME, 2010), while N₂O emissions due to emissions of ammonia and
180 nitric oxide were calculated as 1% of the latter fluxes, as simulated by CERES-EGC. In the
181 ADEME methodology, nitrate leaching was given the same value for all crops except winter

182 oilseed rape, for which specific field references were available. Regarding emissions related
183 to the N content of crop residues, average values were derived from expert knowledge and
184 field surveys, to which a 1% emission factor was applied, in accordance with Eggleston et al.
185 (2006).

186

187 2.2 3. *Life-cycle inventories and impact characterization*

188 Table 1 summarizes the sources of data used for the various steps of the biofuel chains. Crop
189 management data were taken from surveys carried out by the French Ministry of Agriculture
190 in 2006 for arable crops (Gabrielle et al., 2012), and expert knowledge for miscanthus in
191 Northern France (Bessou, 2009; Table 2). The main agricultural inputs are listed in Table 3.
192 Miscanthus was considered unfertilized, but the N exports in harvested biomass were
193 compensated for by adding a corresponding consumption of synthetic fertilizer N to the
194 feedstock production system. Grain yields were obtained from regional simulations by
195 CERES-EGC for arable crops, while miscanthus yields were calculated as 90% of the
196 biomass simulated in late winter, correspond to a late harvest (Strullu et al., 2011). The
197 remaining 10% was returned to the soil as harvest residues.

198 Direct emissions of reactive N (Nr), whether gaseous or leaching, were simulated at regional
199 scale with CERES-EGC over the 2010-2030 time period, along with C and water balances.
200 The predicted Nr losses included: nitrate leaching, emissions of ammonia, nitric oxide and
201 nitrous oxide. Annual arable crops were included in the single following rotation,
202 representative of current crop successions in the area: oilseed rape – winter wheat – sugar-
203 beet - winter wheat - winter barley. For each crop in the rotation, daily simulated fluxes were
204 accumulated from its sowing to the sowing of the following crop. Miscanthus was simulated
205 as a single cycle from planting in 2010 to removal or re-establishment in 2030. Emission
206 fluxes were averaged over the various cropping periods and expressed on a yearly basis for all

17

18

207 crops. Fluxes were spatially averaged on the basis of the land area occupied by each crop or
208 fallow, and a 5%-95% inter-quartile range was calculated from the distribution of emissions
209 per ha in the relevant spatial simulation units, to derive a confidence interval in the LCA.

210

211 Data on biomass conversion to biofuels were taken from various sources relevant to France or
212 Europe (Table 1). Feed co-products of 1st generation biofuels were handled by system
213 expansion using data from Lehuger et al. (2009) on soybean meal from Brazil, as a substitute
214 for either rapeseed meal or dried distillers grains with solubles (DDGS) from wheat, and
215 silage maize, as a substitute for sugar-beet pulp. Other co-products were dealt with by
216 economic allocation (Jungbluth et al., 2007).

217 Rape methyl-ester (or bio-diesel) was produced from the esterification of rapeseed oil with
218 fossile-based methanol, involving glycerin and potassium sulfate as co-products. Data for the
219 conversion of sugar-beet to ethanol were taken from 2 plants located in the Champagne-
220 Ardennes and Picardy regions about 200 kms to the North of Ile de France, considered
221 representative of current best technologies (Bessou, 2009). The conversion of wheat to
222 ethanol involved dry-milling of wheat grains, saccharification and fermentation, and
223 distillation to produce hydrated ethanol (95% basis). The production of the DDGS co-product
224 from stillage included draff separation, concentration, drying and pelletization. The
225 conversion of lignocellulose to ethanol involved steam pre-treatment of biomass,
226 simultaneous saccharification and fermentation of the resulting mash, and distillation to
227 hydrated ethanol. The vinasses produced by the fermentation process were digested to
228 produce biogas and process heat and power. The data originally applied to a pilot plant using
229 grass feedstock but we considered the latter could be replaced by miscanthus biomass due to
230 the relative close chemical compositions of both feedstocks. In addition to ethanol, the
231 process produced proteins and fibres and an economic allocation was made between the 3

19

20

232 end-products (Jungbluth et al., 2007).

233 Environmental impacts were characterized using the CML 2000 at mid-point level (Guinée et
234 al., 2002). The following impact categories were analyzed: eutrophication, acidification,
235 photochemical ozone formation, global warming, and depletion of abiotic resources. The
236 sensitivity of the global warming indicators to the spatial and temporal variations of N₂O
237 emissions in Ile de France was examined by calculating the GHG emissions of biofuels with
238 the median and 5-95% inter-quartile range of these fluxes. LCA calculations were carried out
239 with the Sima Pro software package (v7.1, Pré Consultants, Amersfoort, NL).

240 **3. Results & Discussion**

241 *3.1 Field emissions of reactive N and soil C variations*

242 Table 3 lists the field emissions of reactive N (Nr) and soil organic C (SOC) variations for the
243 various feedstocks obtained with the ecosystem model CERES-EGC. Crop yields predicted in
244 2007, the reference year for the verification of N₂O fluxes (Gabrielle et al., 2012) are
245 compared to statistics reported by the Ministry of Agriculture for the same year. Modelled and
246 observed yields differed by less than for 5% for winter wheat and oilseed rape, but CERES-
247 EGC over-estimated the yields of sugar-beet by 22%. However, the sugar-beet yields
248 averaged over the 2010-2030 simulations were closer to the values reported in 2007 (87 t
249 fresh tuber weight (FW) ha⁻¹ vs. 82 t FW ha⁻¹), which mitigates the possibility of a model bias
250 for sugar-beet. For comparison, sugar-beet yields ranged between 85 and 100 t FW ha⁻¹ over
251 the 2007-2012 period according to the regional agricultural statistics. For winter wheat, the
252 2010-2030 yields predicted by CERES-EGC were similar to the 2007 value (at 7.53 vs. 7.87 t
253 grain dry matter (DM) ha⁻¹), while they were 30% higher for oilseed rape. This increase for
254 rapeseed is 3 times larger than the projections made by a set of agro-ecosystem models for
255 2030 in one site in Ile de France (Brisson and Levrault, 2011), while for wheat yields the

256 latter predicted a 1 t DM ha⁻¹ increase. These differences with our may due to the fact that no
257 beneficial effects of rising CO₂ concentrations were included in the photosynthesis component
258 of CERES-EGC for either crop, and to differences in the soil properties between our regional
259 map and the particular site modelled by Brisson and Levrault (2011).

260 According to CERES-EGC, the highest direct emissions of N₂O occurred with sugar-beet
261 (Table 2), due to its being a spring crop with fertilizer applications later into spring than the
262 winter-sown crops (wheat and oilseed rape), when soil conditions, in particular its
263 temperature are more conducive to denitrification. The high rate of N returned as crop
264 residues by sugar-beet also explains these large fluxes. The emissions of miscanthus were 2-
265 to 5-fold lower than those of the annual crops, in agreement with Drewer et al. (2012), while
266 winter crops had intermediate emission levels. Except for sugar-beet, the direct emissions of
267 N₂O simulated by CERES-EGC were 2- to 4-fold lower than output by the ADEME
268 methodology. Such pattern was already noted in the verification of 2007 over France, for
269 which the atmospheric inversion suggested emission factors (EF) half lower than the default
270 1% value of the IPCC guidelines for cropland (Gabrielle et al., 2012). Deviations between
271 modelled and IPCC Tier 1 estimates for N₂O have been reported in both directions, depending
272 on local climatic and management conditions. An EF of 0.80% was derived for cropland in
273 China with the DNDC model (Li et al., 2001), while Leip et al. (2011) reported values similar
274 to the IPCC Tier 1 range in Europe, with values around the 1% median in France over the
275 1990-2000 time slice. Here, the annual amounts and seasonal distribution of rainfall were
276 similar between the current and near-future climates in Ile de France, which should not have
277 altered the denitrification patterns. Therefore, the low emission levels simulated over 2010-
278 2030 in Ile de France compared to 2007 or other estimates were probably not due to changes
279 in climate forcing.

280 Indirect emissions of N₂O due to leaching or gaseous losses of Nr, as well as the fate of crop
23

281 residues, differed even more markedly between the 2 estimation methodologies (Table 4). The
282 overall ranges across crops were larger with the ADEME than with the model-based
283 methodology: 0.71 – 2.80 kg N₂O-N ha⁻¹ yr⁻¹ vs. 0.30-1.78 kg N₂O-N ha⁻¹ yr⁻¹, respectively.
284 Most of the variations arose from the contribution of crop residues, which was included in the
285 direct emissions estimated with CERES-EGC (since the model simulates the fate of harvest
286 residues), while this term reached up to 1.32 kg N₂O-N ha⁻¹ yr⁻¹ for sugar-beet due to the large
287 N content of the green leaves returned to soils at harvest. This was also captures in the model
288 simulations, as mentioned above. Indirect emissions due to nitrate leaching were similar
289 across the 2 approaches, with the exception of oilseed rape for which the model simulated
290 extremely low nitrate losses.

291 As a consequence, the ranking of crops varied according to the N₂O flux estimation methods:
292 according to ADEME, annual crops had very similar emission rates, around 2.8 kg N₂O-N ha⁻¹
293 yr⁻¹, while miscanthus emitted 4 times less. Conversely, the modelled efflux from oilseed rape
294 was close to that of miscanthus (less than 0.5 kg N₂O-N ha⁻¹ yr⁻¹), while the other 2 annual
295 crops emitted about 3 times more N₂O, with sugar-beet in the upper end. The same pattern
296 applied to nitrate leaching rates, with winter wheat resulting in the highest losses (at 37 kg
297 NO₃-N ha⁻¹ yr⁻¹). The leaching rate from wheat was close to the 40 kg NO₃-N ha⁻¹ yr⁻¹ estimate
298 given by ADEME (2010) as a flat rate for all annual crops except sugar-beet (with a value of
299 18 kg NO₃-N ha⁻¹ yr⁻¹ derived from lysimeter studies). The low leaching rates (under 10 kg
300 NO₃-N ha⁻¹ yr⁻¹) simulated by CERES-EGC with winter oilseed rape arose from the capacity
301 of this crop to take up N in fall. Similarly, the sowing of catch crops or the regeneration of
302 volunteers, in particular before the sowing of the sugar-beet crop could have reduced the
303 losses of nitrate overwinter several-fold (McDonald et al., 2005).

304 Gaseous emissions of NO were in the in the 0.4 – 1.0 kg NO-N ha⁻¹ yr⁻¹ range for annual crops
305 and twice lower for miscanthus (Table 3). Similarly to N₂O, these values are under the 1-2 kg

306 NO-N ha⁻¹ yr⁻¹ range reported by Stehfest and Bouwman (2006) for cropland in Ile de France,
307 using regionalized emission factors and a large data set of field observations. However, in
308 previous tests against field data in the same area, the CERES-EGC model did not reveal any
309 systematic bias in the prediction of NO emissions (Rolland et al., 2008). Regarding ammonia
310 (NH₃), the model simulated net emissions in the 2.3 – 5.1 kg NH₃-N ha⁻¹ yr⁻¹ range for annual
311 crops, and a very small net deposition rate (-0.2 kg NH₃-N ha⁻¹ yr⁻¹) for miscanthus. Overall,
312 simulated gaseous losses of ammonia and nitric oxide were several-fold lower than the IPCC
313 Tier 1 estimate, making up 10% of the fertilizer N inputs (for synthetic fertilizers). However,
314 the modelled estimates are in line with the lower end of this emission factor, at 3% (Eggleston
315 et al., 2006).

316 While there were no significant trends in terms of soil organic carbon (SOC) storage for
317 annual crops, with rates in the -34 to +41 kg C ha⁻¹ yr⁻¹ range, miscanthus had a large capacity
318 to sequester C, with rates around 575 kg C ha⁻¹ yr⁻¹. The latter is in line with multiple long-
319 term studies on miscanthus stands and the 680 kg C ha⁻¹ yr⁻¹ value reported in the review of
320 Don et al. (2011) under stands more than 10 years old. This increase mainly reflected a build-
321 up of soil organic matter due to large rates of litter inputs, combined with the protective effect
322 of reduced tillage.

323

324 *3.2 Life-cycle impacts of feedstock production*

325 Figure 1 compares the impacts of the various candidate energy crops on a hectare (ha) and MJ
326 of feedstock energy content basis. Direct land-use change effects were excluded for
327 miscanthus in this analysis. The annual food crops (wheat, oilseed rape and sugar-beet) had
328 the highest impacts per ha due to their high requirements in agricultural inputs compared to
329 miscanthus, resulting in 60% to 85% lower impacts for the latter. Such pattern was noted by

27

28

330 Monti et al. (2009) in Northern Italy, although to a lower extent, with 50% to 60% lower LCA
331 impacts with miscanthus compared to a wheat-maize rotation on a ha basis.

332 The ranking among the 3 annual crops varied according to the indicator considered. The
333 abiotic depletion (AD) and ozone formation potential (OFP) indicators were within a 10%
334 relative range for all crops, while winter wheat and oilseed rape had 15% lower global
335 warming potentials (GWP) compared to sugar-beet. Oilseed rape had 25% and 60% lower
336 impacts than the other 2 annual crops due to its much low nitrate leaching rates in the field.
337 Overall, most of the differences in LCA impacts on a ha basis arose from the variations in Nr
338 emission patterns across feedstocks.

339 Differences across crops were less pronounced when using one MJ of feedstock energy
340 content (including grains and straw for annual crops) as a functional unit (Figure 1). The
341 highest impacts generally occurred with winter wheat, except for the OFP which was slightly
342 larger with winter wheat. Sugar-beet had overall lower impacts than oilseed rape and wheat,
343 due its 40% higher energy yield per ha (Table 3). Similarly to the results per ha, the impacts of
344 miscanthus per MJ were 80 to 98% lower than the annual crops, given that its energy output
345 per ha was in the upper range of the crops. Overall, crops with a high energy output per ha
346 (such as sugar beet and miscanthus) had comparably lower impacts per MJ than the others,
347 showing that energy yields predominated in the trade-off between high productivity, fertilizer
348 requirements and N₂O emission rates. Miscanthus performed best because it minimized this
349 trade-off. The compensation of N exports by synthetic fertilizers accounted for 10 to 50% of
350 the LCA impacts. Many miscanthus fields in France or the UK are currently unfertilized but is
351 likely to lead to the depletion of soil nutrients in the long-run (Strullu et al., 2011). Prior land
352 use (cropland versus fallow) played a negligible role, bearing in mind that the effects on soil
353 C dynamics were not included at this stage and thus the differences between the two scenarios
354 only reflected variations in terms of soil distribution over Ile de France.

355

356 *3.3 Life-cycle impacts of biofuel chains*

357 Figure 2 reports the GHG emissions of the various biofuel chains investigated here, compared
358 to their fossile equivalents. When excluding land-use change effects (ie on an attributionnal
359 basis), all biofuel chains emitted less GHG than the fossile fuels, with savings ranging from
360 50% (ethanol from winter wheat) to 80% (cellulosic ethanol). For the 1st generation biofuels,
361 the figures based on modelled field emissions (referred to as CERES) were slightly lower than
362 those based on default emission factors (ADEME). The lower field N₂O emission rates with
363 the former methodology were in a large part compensated for by the differences in co-product
364 handling: system expansion with CERES vs. energy-based allocations for ADEME. The latter
365 generally results in a lower environmental burden on biofuels than the former (Cherubini,
366 2010). The GHG emissions of miscanthus-based ethanol were only 60% lower than those of
367 sugar-beet ethanol (the 1st generation chain with the lowest emissions), and 75% lower than
368 the other biofuels. This gap is larger than with the feedstock data (Figure 1) because of the
369 relatively high biomass-to-ethanol yield hypothesized in the conversion process due to the
370 economic allocation with the other end-products. This yield is around 0.60 kg ethanol kg⁻¹
371 feedstock DM, higher than the theoretical yield and the 0.24 value proposed by a recent blueprint
372 design for corn stover (Humbird et al., 2011). Thus, changing the allocation system and process design
373 with fewer co-products would probably have resulted in larger impacts for miscanthus ethanol.
374 The GHG balances presented here fell in the middle or lower end of the ranges given by
375 Chum et al. (2011) worldwide: 22-44 g CO₂ eq./MJ for sugar-beet ethanol, 16-70 eq./MJ for
376 wheat ethanol, 5-75 g CO₂ eq./MJ for bio-diesel from plant oils, and -7 to 47 g CO₂ eq./MJ for
377 cellulosic ethanol. Aside from the low Nr emission rates specific to the CERES methodology,
378 this pattern is probably due to the use of recent technologies for conversion (representative of
379 the last decade), and biomass yields higher than world averages for arable crops.

31

32

380 Accounting for direct LUC effects for miscanthus grown on cropland offset most of the life-
381 cycle emissions due to the high capacity of this perennial grass to sequester C with respect to
382 arable crops (Table 2), resulting in a net value close to the bottom end of the range from
383 Chum et al. (2011). The inclusion of ecosystem C pools in LCA and in particular the effects
384 of land-use and management practices on soil organic C dynamics has been shown to exert a
385 large influence on the GHG abatements of bioenergy. A case-study for miscanthus in the UK
386 concluded to a potential for negative emissions under $-40 \text{ g CO}_2 \text{ eq. MJ}^{-1}$ (Davis et al., 2013).
387 Including indirect LUC effects dramatically altered the GHG savings of all biofuels, including
388 cellulosic ethanol from feedstock grown on cropland (Figure 2). It resulted in negative values
389 for bio-diesel and wheat ethanol, and divided the savings by 2 for sugar-beet and miscanthus-
390 based ethanol grown on cropland, compared to attributional values. Such patterns are
391 common in the literature on consequential LCA, whether based on macro-economic sectoral
392 modelling or simpler substitution and displacement schemes (De Cara et al., 2012;
393 Silalertruksa et al., 2009). For cassava-based ethanol in Thailand, the latter authors cited
394 LUC-related GHG emissions in the 20% to 90% range compared to attributional values,
395 depending on the crops displaced and crop production regions.

396 The uncertainty on N_2O emissions due to their temporal and spatial variability in Ile de France
397 resulted in asymmetric confidence intervals (5%-95%) for the net GHG balance of biofuels,
398 with a magnitude ranging from 2 to 25 $\text{g CO}_2 \text{ eq./MJ}$. This value was largest with wheat
399 ethanol and bio-diesel. The fact that the confidence intervals of these 2 biofuels overlapped
400 indicate that their net GHG emissions were not significantly different. Conversely, the
401 differences between cellulosic ethanol, sugar-beet ethanol and the other 2 biofuels were
402 significant ($p > 0.9$). In their uncertainty analyses on the influence of N_2O emissions on the
403 GHG balances of biofuels, Smeets et al. (2009) reported much larger confidence intervals,
404 similar to life-cycle totals for ethanol from wheat or bio-diesel from oilseed rape. This arose

405 from the large uncertainties on field emissions (ranging from 1 to 4 kg kg N₂O-N ha⁻¹ yr⁻¹ for
406 winter wheat in Europe), and emphasizes the benefits of regional modelling to reduce the
407 magnitude of this uncertainty.

408 Figure 3 shows the LCA results of biofuel chains for a broader range of impact categories. As
409 could be expected from the feedstock comparison, miscanthus ethanol had the lowest impacts,
410 whether established on cropland or fallow. Compared to gasoline, cellulosic ethanol had an 8-
411 fold lower acidification potential but a 5-fold larger impact for eutrophication (ADEME,
412 2010). The LCA results based on ecosystem modelling (CERES) were generally lower than
413 those obtained with the fixed emission factors (ADEME), by a factor of up to ten. These gaps
414 were much larger than for the GHG emissions because feedstock production was the top
415 contributor to these impacts, and the relative differences between ADEME and CERES were
416 in a similar range for Nr emissions (Table 3). Differences between 1st generation biofuels were
417 more pronounced with the ADEME methodology.

418 Overall, sugar-beet ethanol performed better than wheat ethanol and bio-diesel, except for
419 eutrophication for which bio-diesel and miscanthus ethanol were on a par according to the
420 CERES estimation, due to similar nitrate leaching rates. Only a few published LCAs of
421 biofuels include impacts other than GHG emissions or fossile energy consumption. They
422 generally conclude to the same pattern as evidenced here, with short-range impacts such as
423 eutrophication, ozone formation or acidification potentials being larger with biofuels than
424 their fossile counterparts due to Nr emissions upon feedstock cultivation (Gabrielle and
425 Gagnaire, 2008). However, in the case of lignocellulosic plants such as miscanthus, co-
426 benefits in terms of control soil erosion or nutrients filtering have also been pointed out
427 (Chum et al., 2011). At the field- and landscape scales, management practices such as cover
428 crops and buffer zones may thus be introduced to mitigate these local impacts and optimize
429 biofuel chains (Davis et al., 2013; Bessou, 2009). These options may be investigated using the

430 regional modelling systems presented here at the plot-scale, and with the use of integrated
431 landscape models (Dufossé et al., 2013).

432 Overall, sugar-beet ethanol thus emerged as the 1st generation biofuel with the best
433 performance due to its high energy output per unit area, and miscanthus ethanol was still more
434 efficient at abating GHG emissions while minimizing local impacts. Establishing miscanthus
435 on fallow land proved the best option, but is limited in practice by the availability of fallow
436 land in Ile de France (which only makes up 4% of the utilizable arable area in the region). It
437 should also be borne in mind that the data on miscanthus conversion to ethanol is based on an
438 extrapolation of laboratory-scale processes, thus still fraught with a large uncertainty and
439 more prospective in nature. Its results should therefore be considered as indicative rather than
440 representative of a commercial plant. Results from currently-operating pilots should help
441 improve life-cycle inventory data for this process in a near future.

442

443 **4. Conclusion**

444 We assessed the environmental impacts of several biofuel feedstocks and pathways at the
445 regional scale, based on either annual or perennial crops. The use of an ecosystem model to
446 estimate for the emissions of reactive N, as opposed to fixed emission factors, lead to a 5% to
447 15% reduction in the overall GHG emissions of biofuels, due to local soil and climatic
448 characteristics. The GHG savings incurred by the substitution of fossile fuels with biofuels
449 hinged on land-use change scenarios and biofuel pathways, being highest for cellulosic
450 ethanol and lowest for bio-diesel from oilseed rape.

451 ***Acknowledgements***

452 These results were obtained in the framework of the IMAGINE project funded by the
453 ENERBIO programme of the TUCK foundation (Rueil-Malmaison, France).

454 **References**

- 455 1. ADEME, 2010. Life-cycle assessment applied to the first-generation biofuels
456 consumed in France. Final report, BioIS/ADEME, Angers (in French).
- 457 2. Bessou, C. Greenhouse gas emissions of biofuels, Improving Life Cycle Assessments
458 by taking into account local production factors. PhD thesis, AgroParisTech, Paris,
459 2009.
- 460 3. Brisson, N., Levraut, F. (eds), 2011. The Green Book of the CLIMATOR project.
461 ADEME Editions, Angers, France.
- 462 4. Chen, Y., Churkina, G., Heimann, M., 2009. Constructing a consistent historical
463 climate data set for the European domain. Max-Planck Institute for Biogeochemistry,
464 Iena, Technical Report 15 (ISSN 1615-7400).
- 465 3. Cherubini, F., 2010. GHG balances of bioenergy systems - Overview of key steps in
466 the production chain and methodological concerns. *Renew. Energy* 35, 1565-1573.
- 467 4. Chum H., Faaij, A.P.C., Moreira, J., Berndes, G., Dhamija, P., Dong, H., et al., 2011.
468 Bioenergy, in: Edenhofer, O., Pichs-Madruga, R., Sokona, Y., Seyboth, K., Matschoss,
469 P., Kadnert, S. et al. (Eds.) IPCC Special Report on Renewable Energy Sources and
470 Climate Change Mitigation, Cambridge University Press, Cambridge, United
471 Kingdom and New York, NY, USA.
- 472 5. Crutzen, P.J., Mosier, A.R., Smith, K.A., Winiwarter, W., 2008. N₂O release from
473 agro-biofuel production negates global warming reduction by replacing fossil fuels.
474 *Atmos. Chem. Phys.* 8, 385-389.
- 475 6. Davis, S.C., Boddey, R.M., Alves, B.J.R., Cowie, A.L., George, B.H., Ogle, S.M.,
476 Smith, P., van Noordwijk, M., van Wijk, M.T., 2013. Management swing potential for

41

42

- 477 bioenergy crops. GCB Bioenergy (in press).
- 478 7. De Cara, S., Goussebaïle, A., Grateau, R., Levert, F., Quinemer, J., Vermont, B., 2012.
479 Critical review of literature references on the effect of land-use changes on the
480 environmental balances of biofuels. ADEME, Angers, France (in French).
- 481 8. Don, A., Osborne, B., Hastings, A., Skiba, U., Carter, M.S., Drewer, J., Flessa, H.,
482 Freibauer, A., Hyvönen, N., Jones, M.B., Lanigan, G.J., Mander, Ü., Monti, A.,
483 Djomo, S.N., Valentine, J., Walter, K., Zegada-Lizarazu, W., Zenone, T., 2011. Land-
484 use change to bioenergy production in Europe: implications for the greenhouse gas
485 balance and soil carbon. GCB Bioenergy 4, 372–391.
- 486 9. Drewer, J., Finch, J.W., Lloyd, C.R., Baggs, E.M., Skiba, U., 2012. How do soil
487 emissions of N₂O, CH₄ and CO₂ from perennial bioenergy crops differ from arable
488 annual crops? GCB Bioenergy 4, 408–419.
- 489 10. Dufossé, K., Gabrielle, B., Drouet, J.-L., Bessou, C., 2013. Using agroecosystem
490 modelling to improve the estimates of N₂O emissions in the life-cycle assessment of
491 biofuels. Waste and biomass valorization (in press).
- 492 11. Eggleston, H.S., Buendia, L., Miwa, K., Ngara, T., Tanabe K., 2006. IPCC Guidelines
493 for National Greenhouse Gas Inventories, prepared by the National Greenhouse Gas
494 Inventories Programme, IGES, Japan.
- 495 12. Farrell, A.E., Plevin, R.J., Turner, B.T., Jones, A.D., O'Hare, M., Kammen, D.M.,
496 2006. Ethanol can contribute to energy and environmental goals. Science 311, 506-
497 508.
- 498 13. Fargione, J., Hill, J., Tilman, D., Polasky, S., Hawthorne, P., 2008. Land Clearing and
499 the Biofuel Carbon Debt. Science 319, 1235-1237.
- 500 14. Gabrielle, B., Gagnaire, N., 2008. Life-cycle assessment of straw use in bio-ethanol
43

- 501 production: a case-study based on deterministic modelling. *Biomass Bioenergy* 32,
502 431-441.
- 503 15. Gabrielle, B., Boukari, E., Bousquet, P., Gagnaire, N., Goglio, P., Grossel, A.,
504 Lehuger, S., Lopez, M., Massad, R., Nicoullaud, B., Pison, I., Prieur, V., Python, Y.,
505 Schmidt, M., Schulz, M., Thompson, R., 2012. Improved Assessment of the
506 Greenhouse gas balance of bioenergy pathways (IMAGINE). Final project report,
507 UMR EGC AgroParisTech INRA, Thiverval-Grignon. URL: [http://www4.versailles-](http://www4.versailles-grignon.inra.fr/var/internet_versailles_egc/storage/htmlarea/Productions/Gabrielle_B/Rpfinal_IMAGINE_Octobre2012.pdf)
508 [grignon.inra.fr/var/internet_versailles_egc/storage/htmlarea/Productions/Gabrielle B/](http://www4.versailles-grignon.inra.fr/var/internet_versailles_egc/storage/htmlarea/Productions/Gabrielle_B/Rpfinal_IMAGINE_Octobre2012.pdf)
509 [Rpfinal_IMAGINE_Octobre2012.pdf](http://www4.versailles-grignon.inra.fr/var/internet_versailles_egc/storage/htmlarea/Productions/Gabrielle_B/Rpfinal_IMAGINE_Octobre2012.pdf) (last accessed 28 May 2013).
- 510 16. Goglio, P., Colnenne-David, C., Laville, P., Doré, T., Gabrielle, B., 2013. 29% N₂O
511 emission reduction from a modelled low-greenhouse gas cropping system during
512 2009–2011. *Environ. Chemistry Letters* (in press).
- 513 17. Guinée, J.B., Gorrae, M., Heijungs, R., Huppes, G., Kleijn, R., de Koning, A., van
514 Oers, L., Sleswijk, A.W., Suh, S., de Haes, H.A.U., de Bruijn, H., van Duin, R.,
515 Huijbregts, M.A.J., 2002. Handbook of life-cycle assessment. Operational guide to
516 ISO standards. Kluwer Academic Publisher, Dordrecht.
- 517 18. Humbird, D., Davis, R., Tao, L., Kinchin, C., Hsu, D., Aden, A., Schoen, P., Lukas, J.,
518 Olthof, B., Worley, M., Sexton, D., Dudgeon, D., 2011. Process Design and
519 Economics for Biochemical Conversion of Lignocellulosic Biomass to Ethanol.
520 Dilute-Acid Pretreatment and Enzymatic Hydrolysis of Corn Stover. Technical Report,
521 NREL, Golden, Colorado.
- 522 19. In Numeri, 2012. A retrospective analysis of the interactions between biofuel
523 developments and the dynamics of international markets world (agricultural
524 commodities, end-products and co-products) and land-use changes in France.

- 525 ADEME, Angers, France (in French).
- 526 20. Jungbluth, N., Emmenegger, M., Dinkel, F., Stettler, C., Doka, G., Chudacoff, M.,
527 Dauriat, A., Gnansounou, E., Spielmann, M., Sutter, J., Kljun, N., Keller, M., Schleiss,
528 K., 2007. Life Cycle Inventories of Bioenergy Data v2.0. Swiss Centre for Life Cycle
529 Inventories, Switzerland.
- 530 21. Kavanagh, E. (editor), 2006. Looking at biofuels and bioenergy – Commentary.
531 Science 312, 1743-1748.
- 532 22. Lémond, J., Dandin, P., Planton, S., Vautard, R., Pagé, C., Déqué, M., Franchistéguy,
533 L., Geindre, S., Kerdoncuff, M., Li, L., Moisselin, J.-M., Noël, T., Tourre, Y.M., 2011.
534 DRIAS – A step toward French Climate Services. Adv. Sci. Res. 6, 179–186.
- 535 23. Lehuger, S., Gabrielle, B., Gagnaire, N., 2009. Environmental impact of the
536 substitution of imported soybean meal with locally-produced rapeseed meal in dairy
537 cow feed. J. Cleaner Prod. 17, 616-624.
- 538 24. Li, C., Zhuang, Y., Cao, M., Crill, P., Dai, Z., Frohking, S., Moore, III, B., Salas, W.,
539 Song, W., Wang, X., 2001. Comparing a process-based agro-ecosystem model to the
540 IPCC methodology for developing a national inventory of N₂O emissions from arable
541 lands in China. Nutr. Cycl. Agroecosys. 60, 159-175.
- 542 25. Leip, A., Busto, M., Winiwarter, W., 2011. Developing spatially stratified N₂O
543 emission factors for Europe. Environ. Poll. 159, 3223-3232.
- 544 26. MacDonald, A., Poulton, P., Howe, M., Goulding, K., Powlson, D., 2005. The use of
545 cover crops in cereal-based cropping systems to control nitrate leaching in SE England
546 Plant and Soil 273, 355-373.

- 547 27. Monti, A., Fazio, S., Venturi, G., 2009. Cradle-to-farm gate life cycle assessment in
548 perennial energy crops. *Eur. J. Agron.* 31, 77-84.
- 549 28. Picoche, C. Perennial crop modeling with an agro-ecosystem model. Master's
550 dissertation, INSA Lyon, France.
- 551 29. Rolland, M.-N., Gabrielle, B., Laville, P., Cellier, P., Serça, D., Cortinovis, J., 2008.
552 Modeling of nitric oxide emissions from temperate agricultural ecosystems. *Nutr.*
553 *Cycl. Agroecosyst.* 80, 75-93.
- 554 30. Silalertruksa, T., Gheewala, S.H., Sagisaka, M., 2009. Impacts of Thai bio-ethanol
555 policy target on land use and greenhouse gas emissions. *Applied Energy* 86, S170-
556 S177.
- 557 31. Smeets, E.M.W., Bouwman, L.F., Stehfest, E., Van Vuuren, D.P., Posthuma, A., 2009.
558 Contribution of N₂O to the greenhouse gas balance of first-generation biofuels. *Global*
559 *Change Biol.* 15, 1-23.
- 560 32. Stehfest, E., Bouwman, L., 2006. N₂O and NO emission from agricultural vegetation:
561 summarizing available of global annual emissions. *Nutr. Cycl. Agroecosyst.* 74, 207-
562 228.
- 563 33. Strullu, L., Cadoux, S., Preudhomme, M., Jeuffroy, M.-H., Beaudoin, N., 2011.
564 Biomass production and nitrogen accumulation and remobilisation by *Miscanthus*
565 *giganteus* as influenced by nitrogen stocks in belowground organs. *Field Crops Res.*
566 121, 381-391.
- 567 34. Thompson, R.L., Gerbig, C., Rödenbeck, C., 2011. A Bayesian inversion estimate of
568 N₂O emissions for western and central Europe and the assessment of aggregation
569 errors. *Atmos. Chem. Phys.* 11, 3443–3458.

570 Figure captions

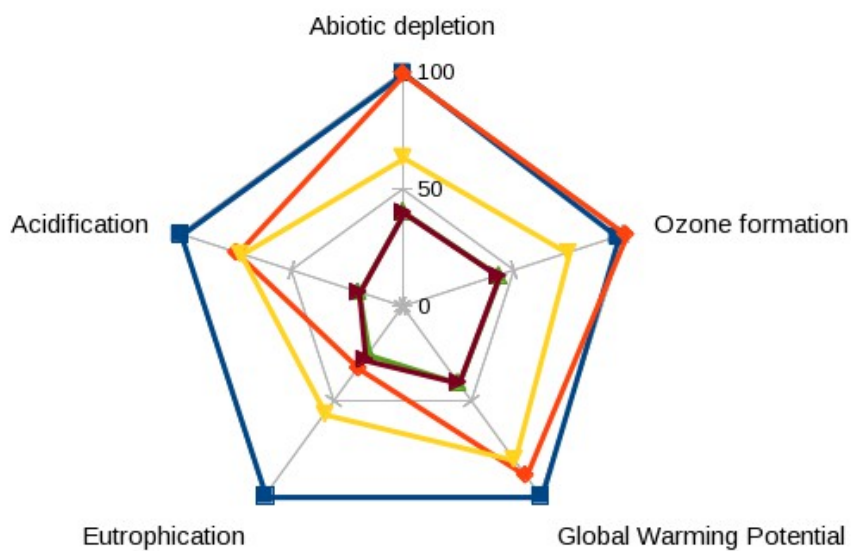
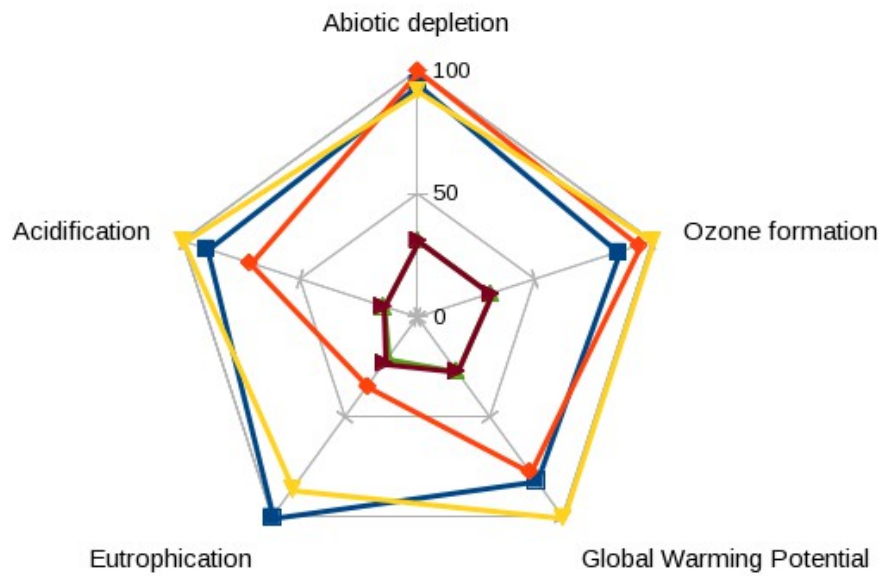
571

572 Figure 1. Compared cradle-to-farm-gate LCA results for the various feedstocks per ha (top)
573 and MJ of biofuel feedstock energy content (bottom). Two scenarios were implemented for
574 miscanthus : conversion from cropland or fallow land. Direct effects of land-use changes are
575 excluded here.

576 Figure 2. Life-cycle emissions of greenhouse gases per MJ of of biofuels and their fossile
577 equivalents. EtOH : ethanol, RME: rape methyl-ester; W: wheat; SB: Sugar-Beet. ADEME
578 refers to the ADEME 2010 study and methodology, and CERES to the modelled emissions of
579 Nr. Emissions related to direct and indirect land-use changes are noted dLUC and iLUC,
580 respectively. The error bars correspond to the 5%-95% confidence intervals with respect to the
581 field emissions of N2O.

582 Figure 3. Relative life-cycle impacts of biofuels in Ile de France using either regional
583 ecosystem modelling (CERES) or IPCC Tier 1 emission factors (ADEME), per MJ of biofuel
584 energy content. EtOH : ethanol, RME: rape methyl-ester; SB: Sugar-Beet; Misc: miscanthus.

585



■ Wheat ◆ Oilseed Rape ★ Sugar-Beet
▲ Miscanthus / Cropland ▲ Miscanthus / Fallow

Figure 1. Compared cradle-to-farm-gate LCA results for the various feedstocks per ha (top) and MJ of biofuel feedstock energy content (bottom). Two scenarios were implemented for miscanthus : conversion from cropland or fallow land. Direct effects of land-use changes are excluded here.

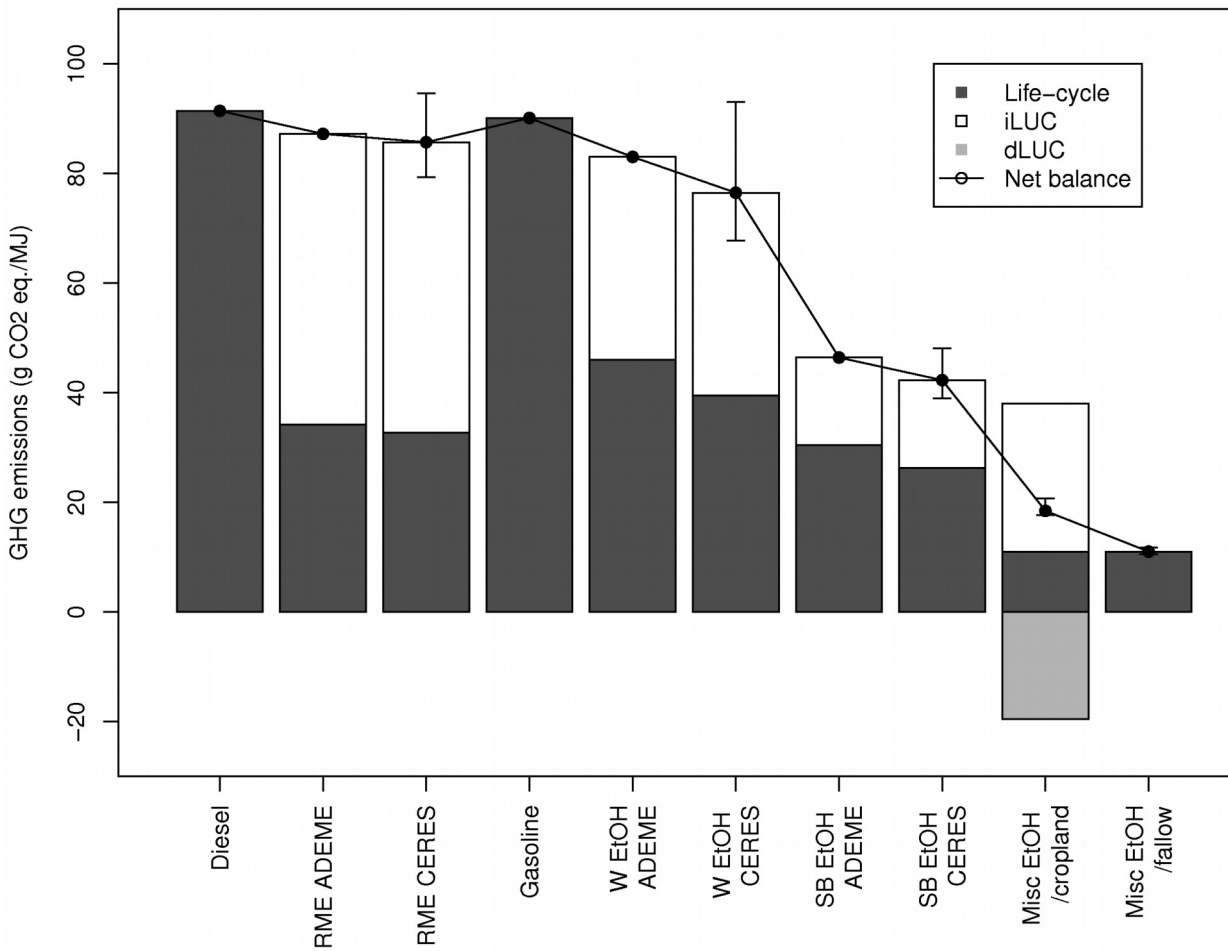


Figure 2. Life-cycle emissions of greenhouse gases per MJ of biofuels and their fossil equivalents. EtOH : ethanol, RME: rape methyl-ester; W: wheat; SB: Sugar-Beet. ADEME refers to the ADEME 2010 study and methodology, and CERES to the modelled emissions of Nr. Emissions related to direct and indirect land-use changes are noted dLUC and iLUC, respectively. The error bars correspond to the 5%-95% confidence intervals with respect to the field emissions of N₂O.

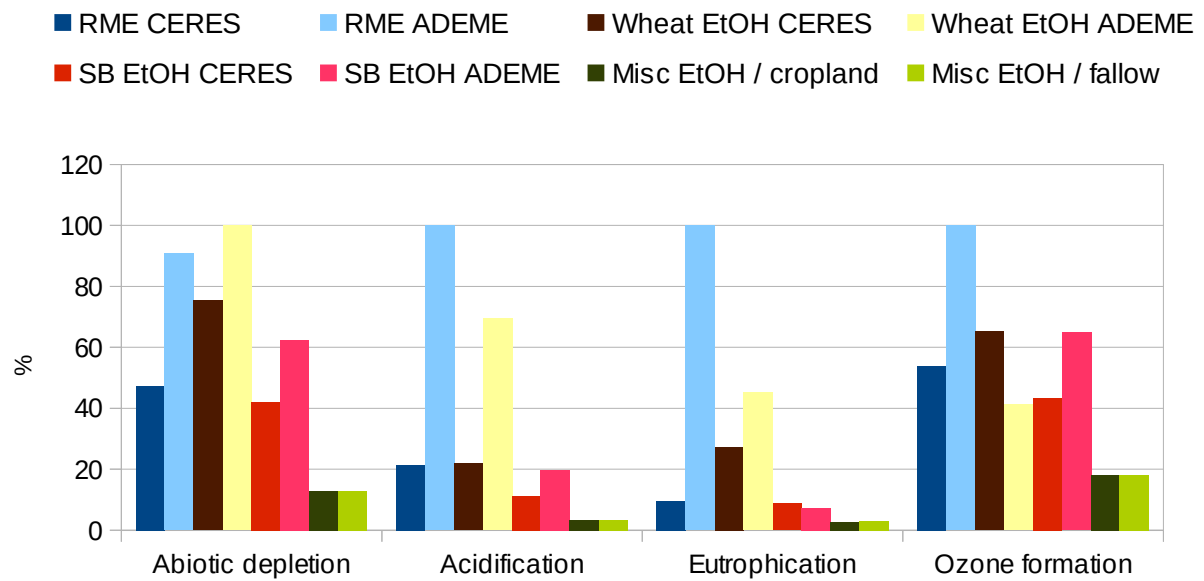


Figure 3. Relative life-cycle impacts of biofuels in Ile de France using either regional ecosystem modelling (CERES) or IPCC Tier 1 emission factors (ADEME), per MJ of biofuel energy content. EtOH : ethanol, RME: rape methyl-ester; SB: Sugar-Beet; Misc: miscanthus.

Processes / stage	Source
Feedstock production	
Crop management data:	
- miscanthus	Expert knowledge ¹
- winter wheat	AGRESTE survey ²
- oilseed rape	AGRESTE survey ²
- sugar-beet	AGRESTE survey ²
Crop yields	CERES-EGC simulations
Machinery & inputs production (fertilizers, pesticides, fuel)	EcoInvent database (v2.0) ³
Field emissions	
N ₂ O emissions	IPCC 2006 guidelines, CERES-EGC or O-CN simulations
Other direct Nr losses	CERES-EGC simulations
Soil C dynamics	IPCC guidelines or CERES-EGC simulations
Transport	EcoInvent database
Conversion to biofuel	
1 st generation biofuels	EcoInvent database, refs 1 and 4
2 nd generation ethanol	EcoInvent database, ref. 1

Table 1. Sources of data for the life-cycle inventory of the pathways investigated. AGRESTE refers to the Statistical Bureau of the French Ministry of Agriculture. References: 1: Bessou, 2009; 2: Gabrielle et al., 2012; 3: Jungbluth et al., 2007 ; 4: ADEME, 2010

	Winter wheat	Sugar Beet	Oilseed Rape	Miscanthus on cropland	Miscanthus on fallow
Fertilizer input rates (kg N-P-K ha ⁻¹)					
Mineral N	200	133	182	0	0
P	28	48	33	2.7	2.7
K	26	160	44	4	4
Pesticide input rates (kg a.i. ha ⁻¹)					
	1.11	1.42	2.48	0.10	0.10
Regional crop yields in 2007 (t DM ha ⁻¹)					
Observed	7.70 ^a	8.50 ^a	3.20 ^a		
CERES-EGC predictions	7.87 (grains)	10.92 (tubers)	3.09 (grains)	14.9 (aerial DM)	14.4 (aerial DM)

593

594 a : from agricultural statistics for 2007

Table 2. Crop management data for the energy crops considered here. DM: dry matter.

595

596

597

61

62

	Winter wheat	Sugar Beet	Oilseed Rape	Miscanthus on cropland	Miscanthus on fallow
N₂O (direct):					
CERES-EGC	1.04	1.49	0.42	0.23	0.23
	(0.11-2.98)	(0.11 – 3.97)	(0.10–0.87)	(0.10 – 0.60)	(0.14 – 0.35)
NO	0.80	0.99	0.86	0.41	0.42
NH ₃	4.10	5.14	2.31	-0.16	-0.16
Nitrate	36.8	30.4	9.4	8.9	10.3
Soil C stock variations (kg C ha⁻¹ yr⁻¹)					
	5	-34	41	575	577
Crop yields (t DM or fresh tuber ha⁻¹)					
	7.53	82.2 ^a	4.19	13.1	13.2
Energy yield, whole-plant basis (GJ ha⁻¹)					
	257	392	274	210	211

a: fresh tuber weight ha⁻¹

Table 3. Nr losses, soil C changes and dry matter (DM) and energy yields for the biofuel feedstocks (area-weighted mean and 5%-95% inter-quartile range in brackets for direct N₂O emissions). Variations in soil C stocks are reported over the 21-year simulation period, as averaged on an annual basis.

	Winter wheat	Sugar Beet	Oilseed Rape	Miscanthus on cropland	Miscanthus on fallow
CERES-EGC :					
- direct	1.04	1.49	0.42	0.23	0.23
- indirect (leaching + gaseous)	0.32	0.29	0.10	0.07	0.08
TOTAL	1.36	1.78	0.52	0.30	0.31
	(0.33-3.30)	(0.40-4.26)	(0.20-0.97)	(0.17-0.67)	(0.22-0.43)
ADEME (2010)					
- direct	2.00	1.33	1.82	0.5	0.5
- indirect :					
harvest residues	0.50	1.32	0.60	0.06 ^c	0.06 ^c
nitrate leaching	0.30	0.13	0.30	0.15 ^b	0.19 ^b
TOTAL	2.80	2.78	2.72	0.71	0.71

599 a : nitrate leaching rates from ADEME (2010)

600 b : nitrate leaching rates from CERES-EGC simulations

601 c : residues left after removal of the miscanthus stand (below-ground N stock estimated at 100

602 kg N ha⁻¹ in late spring ; Strullu et al., 2011).

Table 4. Estimates of N₂O emissions (kg N₂O-N ha⁻¹ yr⁻¹) for the various feedstocks obtained with the agro-ecosystem model CERES-EGC or the IPCC 2006 guidelines (ADEME, 2010).

603

65

66